J. Am. Chem. Soc. **1994,** *116,* 2859–2868

Photochemistry of the Luminescent Alkyl Complexes Alkyl(carbonyl)bis(triarylphosphine)(maleonitrile-dithiolato)iridium, $IrR(CO)(PAr_3)_2(mnt)$

Prudence Bradley, Gianfranco Suardi, Arden P. Zipp, and Richard Eisenberg*

Contribution from the Department of Chemistry, University of Rochester, Rochester, New York 14627

Received August 20, 1993[•]

Abstract: A series of luminescent alkyl complexes of formula $IrR(CO)L_2(mnt)$, where mnt = maleonitriledithiolate, R = Me, Et, Pr, and CH_2CN, and L is a triarylphosphine, have been synthesized and characterized. The complexes possess octahedral coordination geometries with the phosphine ligands in mutually trans positions, as confirmed by a crystal structure determination of the methyl derivative. Crystal data for $IrMe(CO)(PPh_3)_2(mnt)$: $IrS_2P_2ON_2C_{42}H_{33}$, triclinic space group $P\bar{1}$, $a = 13.178(4)$ Å, $b = 13.670(4)$ Å, $c = 12.592(2)$ Å, $\alpha = 105.03(2)°$, $\beta = 115.42(2)°$, $\gamma = 95.72(2)°$, $V = 1919.9$ A^3; $Z = 2$, 6298 reflections (h, $\pm k$, $\pm l$, $4° < 2\theta < 45°$), $R_1 = 0.020$, $R_2 = 0.028$, and GOF = 1.09. The Ir–S distances of 2.442(1) and 2.371(1) Å reflect the structural influence of the trans ligands (Me and CO, respectively). The alkyl complexes luminesce in fluid solution with an emission energy in the range of 695–780 nm and a band shape that suggests vibronic structure characteristic of other mnt complexes. Photolysis of $IrMe(CO)(PPh_3)_2(mnt)$ in the presence of H-atom sources and radical traps leads to products consistent with Ir–alkyl bond homolysis. Further photochemical studies in the presence of ^{13}CO suggest that Ir–Me bond homolysis is favored strongly over CO photodissociation. Photochemistry of $IrR(CO)(PPh_3)_2(mnt)$, where R contains β-hydrogens, produces only the β-elimination products of olefin and the hydride complex $IrH(CO)(PPh_3)_2(mnt)$ even in the presence of large excesses of phosphine, CO, or different radical trapping agents. The quantum yield for photochemical β-elimination of 0.30 is much greater than that determined for photochemical disappearance of $IrMe(CO)L_2(mnt)$ and is consistent with an efficient H-atom transfer from $R^\bullet$ to $^\bullet Ir(CO)L_2(mnt)$ within the radical pair generated by photolysis.

Introduction

The photochemistry of transition-metal complexes containing both carbonyl and σ-bonded alkyl ligands is of interest because these systems possess, in principle, competitive two-electron and one-electron photochemical pathways, with photodissociation of CO being the two-electron path and metal–alkyl bond homolysis the one-electron path. The most studied of these compounds possess the general formula $(\eta^5\text{-}C_5H_5)M(CO)_xR$, where M = Cr, Mo, W, Mn, Fe, and Ru, and the photochemistry and photophysics of these compounds have been reviewed.[1–4]

One of the most detailed studies of these systems is Blaha and Wrighton's report on the photochemistry of $(\eta^5\text{-}C_5R_5)Fe(CO)_2(\eta^1\text{-}CH_2C_6H_5)$, R = H, Me.[5] These complexes were observed to produce 1,2-diphenylethane (bibenzyl) when photolyzed, suggestive of metal–alkyl bond homolysis, but upon further investigation in alkane solutions and 77 K matrices, the complexes were found to photodissociate CO preferentially. In the absence of added CO or PPh_3, the major photochemical process that occurred in a 77 K alkane matrix was loss of CO followed by η^1-Bz-to-η^3-Bz conversion, forming $(\eta^5\text{-}C_5R_5)Fe(CO)(\eta^3\text{-}CH_2C_6H_5)$. The monocarbonyl remained upon warming of the sample to 196 K, but continued warming to room temperature resulted in regeneration of the dicarbonyl. In a later study, photolysis of $(\eta^5\text{-}C_5R_5)Fe(CO)_2(\eta^1\text{-}CH_2C_6H_5)$ in a rigorously purged solution produced $(\eta^5\text{-}C_5R_5)Fe(CO)(\eta^3\text{-}CH_2C_6H_5)$ and $[(\eta^5\text{-}C_5R_5)Fe(CO)_2]_2$[6] in a 10:1 ratio, suggestive of the relative efficiency of CO loss versus bond homolysis in fluid solution at 298 K. Quantum yield measurements of the disappearance of $(\eta^5\text{-}C_5R_5)Fe(CO)_2(\eta^1\text{-}CH_2C_6H_5)$ in the presence and absence of phosphine provided additional support for this conclusion. Thus, the overall photochemistry of $(\eta^5\text{-}C_5R_5)Fe(CO)_2(\eta^1\text{-}CH_2C_6H_5)$ was found to be facile CO photodissociation as the major photochemical process, with a less efficient light-driven homolysis of the Fe–benzyl bond leading to the net observable products of bibenzyl and $[(\eta^5\text{-}C_5R_5)Fe(CO)_2]_2$.

Similar photochemistry has been reported for the related system $(\eta^5\text{-}C_5H_5)W(CO)_3(\eta^1\text{-}CH_2C_6H_5)$,[3b] and these conclusions can be generalized to other $(\eta^5\text{-}C_5R_5)M(CO)_xR$ complexes as well. Recent studies reinforce CO photodissociation as the principal photochemical process in these systems,[7] with the 16-electron intermediates thus formed reacting by addition of other ligands including tertiary phosphines,[8] olefins,[9] and acetylenes[10] and by η^1-to-η^3 conversions of alkenyl ligands.[11]

In this paper, we describe the synthesis, characterization, and photochemistry of a set of Ir(III) alkyl carbonyl complexes. These systems, which have the general formula $IrR(CO)(PR'_3)_2(mnt)$ where mnt = maleonitriledithiolate, were first prepared by us in studying the oxidative addition of alkyl halides to the square-planar anionic complexes $[Ir(CO)(PR'_3)(mnt)]^-$. The triphenylphosphine member of the Ir(I) series, $[Ir(CO)(PPh_3)(mnt)]^-$, had been reported previously by Johnson *et al.*[12] and found to possess a highly structured emission which was assigned as

---

[•] Abstract published in *Advance ACS Abstracts,* March 1, 1994.

(1) (a) Barnett, K. W.; Treichel, P. M. *Inorg. Chem.* **1967**, *6*, 294. (b) Alt, H. G.; Schwarzle, J. A.; Kreiter, C. G. *J. Organomet. Chem.* **1978**, *153*, C7. (c) Severson, R. G.; Wojcicki, A. *J. Organomet. Chem.* **1978**, *153*, 173.

(2) (a) Nesmeyanov, A. V.; Chenskaya, T. B.; Babakina, G. N.; Kritskaya, I. I. *Bull. Acad. Sci. USSR, Div. Chem. Sci.* (*Engl. Transl.*) **1970**, *1129*. (b) Alt, H. G. *J. Organomet. Chem.* **1977**, *124*, 167. (c) Rausch, M. D.; Gismondi, T. E.; Alt, H. G.; Schwarzle, J. A. *Z. Naturforsch.* **1977**, *32b*, 998. (d) Samuel, E.; Rausch, M. D.; Gismondi, T. E.; Mintz, E. A.; Giannotti, C. *J. Organomet. Chem.* **1979**, *172*, 309.

(3) (a) Kazlauskas, R. J.; Wrighton, M. S. *J. Am. Chem. Soc.* **1980**, *102*, 1727. (b) Kazlauskas, R. J.; Wrighton, M. S. *J. Am. Chem. Soc.* **1982**, *104*, 6005. (c) Klein, B.; Kazlauskas, R. J.; Wrighton, M. S. *Organometallics* **1982**, *1*, 1338. (d) Tyler, D. R. *Inorg. Chem.* **1981**, *20*, 2257.

(4) Pourreau, D. B.; Geoffroy, G. L. *Adv. Organomet. Chem.* **1985**, *24*, 249.

(5) Blaha, J. P.; Wrighton, M. S. *J. Am. Chem. Soc.* **1985**, *107*, 2694.

(6) Alt, H. G.; Heberhold, M.; Rausch, M. D.; Edwards, B. H. *Z. Naturforsch,* **1975**, *34b*, 1070.

(7) (a) Mahmoud, K. A.; Rest, A. J.; Alt, H. G. *J. Chem. Soc., Dalton Trans.* **1985**, 1365. (b) Mahmoud, K. A.; Rest, A. J.; Alt, H. G.; Eichner, M. E.; Jansen, B. M. *J. Chem. Soc., Dalton Trans.* **1985**, 175.

0002-7863/94/1516-2859$04.50/0

$^3(d\pi^*_{mnt})$ metal-to-ligand change transfer (MLCT) on the basis of systematic ligand substitution. While the Ir(I) complexes luminesce only in rigid media and the solid state, the six-coordinate RX oxidative addition products were found to emit in fluid solution as well.[13] This unusual feature of the electronic structure of these alkyl carbonyl complexes stimulated the current investigation into their solution photochemistry. The fact that the complexes possessed both carbonyl and alkyl ligands also allowed examination of the relative tendencies of CO photodissociation versus metal–alkyl photohomolysis for a different series of complexes. Preliminary aspects of this work have been reported previously.[13]

Experimental Section

Materials. The following materials were used as received: iridium trichloride hydrate (Johnson Matthey); bis(triphenylphosphoranylidene)ammonium (PPN) chloride, 1-bromo-5-hexene, *tert*-butyl isocyanide, 4-hydroxy-Tempo, iodoacetonitrile, methyl iodide, *n*-propyl iodide, tetra-*n*-butylammonium (TBA) bromide, trifluoroacetic acid, triphenylphosphine (Aldrich); tris(*p*-chlorophenyl)phosphine, tris(*p*-fluorophenyl)phosphine, tris(*p*-methoxyphenyl)phosphine, tris(*p*-tolyl)phosphine (Strem); ethyl iodide, toluene (Eastman); $Fe(NO_3)_3{\cdot}9H_2O$ (Baker Analyzed Reagent); and 60% perchloric acid (Mallinckrodt Analytical Reagent). Sodium maleonitriledithiolate (mnt),[14a] 2-(allyloxy)-1-iodoethane,[14b] 1-iodo-5-hexene,[14c] and Reinecke's salt[15] were prepared according to literature methods. Reagent grade solvents were used for all syntheses; pyridine was distilled from barium oxide. For spectroscopic measurements, chloroform (Baker Photorex) was dried with calcium chloride, a fresh bottle of acetonitrile or methylene chloride (Baker Photorex) was used for each day's measurements, and EPA mixed solvent was prepared from five parts ethyl ether (Baker Photorex), five parts isopentane (Aldrich spectrophotometer grade), and two parts ethanol (Baker Photorex). NMR solvents were purified as follows: benzene-d_6, predried and distilled from calcium hydride onto sodium, stirred overnight, and then vacuum transferred; bromoform-d_1, shaken with activated zinc dust and filtered; acetone-d_6, vacuum transferred from calcium sulfate; and chloroform-d_1, vacuum transferred from molecular sieves after predrying with P_2O_5.

Preparation of Complexes. The complex $TBA[IrBr_2(CO)_2]$ was prepared from iridium trichloride hydrate by an adaptation of the method of Cleare and Griffith[16] and recrystallized from acetone and 2-propanol. The complexes $TBA[Ir(CO)_2(mnt)]$, $TBA[Ir(CO)(PPh_3)(mnt)]$, and $PPN[Ir(CO)_2(mnt)]$ were prepared according to established procedures.[12] All complexes were prepared under a nitrogen atmosphere using standard vacuum line and inert atmosphere techniques. Elemental analyses were performed by Galbraith Laboratories, Inc., Knoxville, TN.

$IrMe(CO)(PPh_3)_2(mnt)$ (1a). $TBA[Ir(CO)_2(mnt)]$ (0.415 g, 0.658 mmol) and PPh_3 (0.401 g, 1.53 mmol) were placed in a flask, and 4 mL of degassed acetone was added. Vigorous evolution of gas followed. The golden orange solution was stirred for 15 min, and 61 μL (0.987 mmol) of MeI was added. The bright yellow solution was stirred for 30 min, and the yellow precipitate that formed was suction filtered in air and washed with hexanes. The filtrate was concentrated to ~2 mL, 4 mL of 2-propanol was added, and the solution was concentrated further. The resulting yellow precipitate was suction filtered and washed with hexanes. Yield, 90%. Anal. Calcd for $IrC_{42}H_{33}N_2OP_2S_2$: C, 56.05; H, 3.70; N, 3.11; P, 6.88; S, 7.13. Found: C, 54.82; H, 3.79; N, 2.98; P, 6.91; S, 7.26.

$IrMe(CO)(P(p\text{-tol})_3)_2(mnt)$ (1b). The same procedure as that used for the preparation of **1a** was employed with the following amounts of materials: $TBA[Ir(CO)_2(mnt)]$, 0.115 g, 0.182 mmol; $P(p\text{-tol})_3$, 0.138 g, 0.455 mmol; and MeI, 17 μL, 0.273 mmol. Yield, 71%.

$IrMe(CO)(P(p\text{-}C_6H_4Cl)_3)_2(mnt)$ (1c). The same procedure as that used for the preparation of **1a** was employed with the following amounts of materials: $TBA[Ir(CO)_2(mnt)]$, 0.239 g, 0.379 mmol; $P(p\text{-}C_6H_4Cl)_3$, 0.158 g, 0.390 mmol; and MeI, 35 μL, 0.568 mmol. Precipitation was effected using hexanes, yielding orange crystals. Yield, 89%.

$IrMe(CO)(P(p\text{-}C_6H_4F)_3)_2(mnt)$ (1d). $TBA[Ir(CO)_2(mnt)]$ (0.184 g, 0.292 mmol) and $P(p\text{-}C_6H_4F)_3$ (0.104 g, 0.299 mmol) were placed in a flask, and 4 mL of acetone was added. Vigorous evolution of gas resulted; the golden orange solution was stirred for 10 min. The solution was concentrated, 3 mL of hexanes was added, and the solution was cooled to −20 °C overnight, resulting in an orange oil upon further removal of solvent. The oil was then taken up in acetone, 50 μL (0.802 mmol) in MeI was added, and the orange-brown solution was stirred for 2 h. $P(p\text{-}C_6H_4F)_3$ (0.135 g, 0.425 mmol) was then added in an acetone solution. After being stirred for 1.5 h, the solution was concentrated to 2.5 mL, and 3 mL of 2-propanol was added. After further concentration of the solution, a precipitate resulted. The precipitate was suction filtered and washed with 2-propanol and hexanes. Yield, 37%. Anal. Calcd for $IrC_{42}H_{27}F_6N_2OP_2S_2$: C, 50.05; H, 2.70; F, 11.31; S, 6.36. Found: C, 50.49; H, 3.63; F, 10.53; S, 6.17.

$IrMe(CO)(P(p\text{-}C_6H_4(OMe))_3)_2(mnt)$ (1e). The same procedure as that used for the preparation of **1a** was employed with the following amounts of materials: $TBA[Ir(CO)_2(mnt)]$, 0.076 g, 0.121 mmol; $P(p\text{-}C_6H_4(OMe))_3$, 0.138 g, 0.455 mmol; and MeI, 12 μL, 0.182 mmol. Yield, 63%.

$IrMe(CO)(CN\text{-}t\text{-}Bu)_2(mnt)$ (1f). $TBA[Ir(CO)_2(mnt)]$ (0.148 g, 0.234 mmol) was placed in a flask, and 5 mL of acetone was added. Addition of 27 μL (0.240 mmol) of *t*-BuNC led to vigorous evolution of gas. The resulting orange solution was stirred for 10 min, and 22 μL (0.351 mmol) of MeI was added. The green-orange solution was stirred for 5 min, and 26 μL (0.234 mmol) of *t*-BuNC was added. The golden yellow solution was stirred for 30 min. After concentration of the solution and addition of 4 mL of 2-propanol, the solution was stored at −20 °C overnight. A bright yellow precipitate resulted, which was suction filtered and washed with 2-propanol and hexanes. Yield, 50%. Anal. Calcd for $IrC_{16}H_{21}N_4OS_2$: C, 35.48; H, 3.91; N, 10.34; s, 11.84. Found: C, 35.53; H, 3.94; N, 10.19; S, 11.97.

$IrEt(CO)(PPh_3)_2(mnt)$ (2a). $TBA[Ir(CO)(PPh_3)(mnt)]$ (0.096 g, 0.111 mmol) was placed in a flask, and 4 mL of degassed acetone was added. Addition of 44 μL (0.535 mmol) of EtI resulted in an orange solution, which was stirred for 4 h. An acetone solution of PPh_3 (0.040 g, 0.144 mmol) was then added. The resulting yellow solution was immediately concentrated, and cold 2-propanol was added to precipitate the ethyl complex. The yellow precipitate was suction filtered and washed with hexanes. Yield, 80%. Anal. Calcd for $IRC_{43}H_{35}N_2OP_2S_2$: C, 56.55; H, 3.86; N, 3.07; P, 6.78. Found: C, 56.14; H, 3.86; N, 2.94; P, 6.62.

$Ir(n\text{-}Pr)(CO)(PPh_3)_2(mnt)$ (3a). This complex was prepared analogously to **2a** using $TBA[Ir(CO)(PPh_3)(mnt)]$ (0.103 g, 0.119 mmol), *n*-PrI (23 μL, 0.239 mmol), and PPh_3 (0.047 g, 0.148 mmol). Yield, 55%.

$Ir(CH_2CN)(CO)(PPh_3)_2(mnt)$ (4a). The same procedure as that used for the preparation of **1a** was employed with the following amounts of materials: $TBA[Ir(CO)_2(mnt)]$, 0.100 g, 0.158 mmol; PPh_3, 0.098 g, 0.374 mmol; and ICH_2CN, 21 μL, 0.535 mmol. Yield, 58%.

$IrH(CO)(PPh_3)_2(mnt)$ (5a). $TBA[Ir(CO)_2(mnt)]$ (0.100 g, 0.159 mmol) and PPh_3 (0.098 g, 0.374 mmol) were placed in a flask, and 4 mL of acetone was added. The yellow-orange solution was stirred for 15 min, and 21 μL (0.268 mmol) of trifluoroacetic acid was added. The bright yellow solution was stirred for 30 min, and the yellow precipitate that formed was suction filtered and washed with ethyl ether. Yield, 81%.

$IrH(CO)(P(p\text{-tol})_3)_2(mnt)$ (5b). $TBA[Ir(CO)(P(p\text{-tol})_3)(mnt)]$ (0.121 g, 0.220 mmol) (prepared analogously to $TBA[Ir(CO)(PPh_3)(mnt)]$[12]) and $P(p\text{-tol})_3$ (0.047 g, 0.119 mmol) were placed in a flask, and 4 mL of acetone was added. Addition of 64 μL (1.10 mmol) of glacial acetic acid resulted in a green-orange solution that was stirred for 2.5 h, at which point IR spectroscopy indicated that equilibrium had been reached. Trifluoroacetic acid (17 μL, 0.22 mmol) was then added. The solution turned bright yellow, and the IR spectrum indicated a complete reaction.

---

[8] See ref 1c and 2. (a) Su, S. R.; Wojcicki, A. *J. Organomet. Chem.* **1971**, *27*, 231. (b) Alt, H. G.; Schwarzle, J. A. *J. Organomet. Chem.* **1978**, *162*, 45. (c) Sim, G. A.; Woodhouse, D. I.; Knox, G. R. *J. Chem. Soc., Dalton Trans.* **1979**, 629.

[9] See ref 1b. (a) Alt, H. G.; Eichner, M. E. *Angew. Chem., Int. Ed. Engl.* **1982**, *21*, 78. (b) Lewis, C.; Wrighton, M. S. *J. Am. Chem. Soc.* **1983**, *105*, 7768.

[10] (a) Alt, H. G. *Angew. Chem., Int. Ed. Engl.* **1976**, *15*, 759. (b) Alt, H. G.; Eichner, M. E.; Jansen, B. M. *Angew. Chem., Int. Ed. Engl.* **1982**, *21*, 861.

[11] See refs 3a,b and 5. (a) Fish, R. W.; Giering, W. D.; Marten, D.; Rosenblum, M. *J. Organomet. Chem.* **1976**, *105*, 101. (b) Kazlauskas, R. J.; Wrighton, M. S. *Organometallics* **1982**, *1*, 602. (c) Su, S. N.; Wojcicki, A. *Organometallics* **1983**, *2*, 1296. (d) Belmont, J. A.; Wrighton, M. S. *Organometallics* **1986**, *5*, 1421.

[12] Johnson, C. E.; Eisenberg, R.; Evans, T. R.; Burberry, M. S. *J. Am. Chem. Soc.* **1983**, *105*, 1795.

[13] Bradley, P.; Johnson, C. E.; Eisenberg, R. *J. Chem. Soc., Chem. Commun.* **1988**, 255.

[14] (a) Davison, A.; Holm, R. H. *Inorg. Synth.* **1967**, *10*, 8. (b) Kinney, R. J.; Jones, W. D.; Bergman, R. G. *J. Am. Chem. Soc.* **1978**, *100*, 7902. (c) Vogel, A. I. *Vogel's Textbook of Practical Organic Chemistry*, 4th ed.; Longman: London, 1978; p 398.

[15] Wegner, E. E.; Adamson, A. W. *J. Am. Chem. Soc.* **1966**, *88*, 394.

[16] Cleare, M. J.; Griffith, W. P. *J. Chem. Soc. A* **1970**, 2788.

Ethyl ether was added to form a precipitate. The resulting yellow solid was suction filtered and washed with ethyl ether. Yield, 70%.

IrH(CO)(PEt$_3$)$_2$(mnt) (5c). TBA[Ir(CO)$_2$(mnt)] (0.406 g, 0.644 mmol) was placed in a flask, and 10 mL of benzene was added. Addition of 500 μL of PEt$_3$ (0.748 mmol) resulted in a red oil and an orange solution. Addition of 55 μL (0.966 mmol) of glacial acetic acid resulted in an orange-yellow solution, which was stirred for 2 h. Addition of 10 mL more of benzene preceded extraction with 10 mL of water. The benzene solution was then placed in a clean flask, and 20 mL of heptane was added. The solution became cloudy and was cooled to −20 °C overnight. The resulting yellow precipitate was cannula filtered and washed with heptane. Yield, 85%. Anal. Calcd for $IrC_{17}H_{31}N_2OP_2S_2$: C, 34.16; H, 5.23; N, 4.69; P, 10.36; S, 10.73. Found: C, 34.16; H, 5.20; N, 4.59; P, 10.35; S, 10.81.

Ir(5-hexenyl)(CO)(PPh$_3$)$_2$(mnt) (6a). TBA[Ir(CO)(PPh$_3$)(mnt)] (0.091 g, 0.105 mmol) was placed in a flask, and 4 mL acetone was added. Addition of 30 μL (0.210 mmol) of 1-iodo-5-hexene resulted in an orange solution, which was stirred for 24 h at 0 °C in the dark. After 24 h, an acetone solution of PPh$_3$ (0.028 g, 0.105 mmol) was added. The resulting yellow solution was immediately concentrated, and 2-propanol was added to precipitate the alkyl complex. The yellow precipitate was suction filtered and washed with hexanes. Yield, 55%.

Ir(2-(allyloxy)ethyl)(CO)(PPh$_3$)$_2$(mnt) (7a). TBA[Ir(CO)(PPh$_3$)(mnt)] (0.072 g, 0.083 mmol) was placed in a flask, and 5 mL of benzene was added with enough acetone, 0.5 mL, to dissolve the iridium complex. Addition of 89 μL (0.416 mmol) or 1-iodo-2-(allyloxy)ethane was followed by addition of 67 μL (0.83 mmol) of pyridine. The resulting orange solution was stirred for 18 h in the dark, and an acetone solution of PPh$_3$ (0.033 g, 0.125 mmol) was added. The resulting yellow solution was immediately concentrated, and 2-propanol was added to precipitate the alkyl complex. The yellow precipitate was suction filtered and washed with hexanes. Yield, 73%.

IrBr(CO)(PPh$_3$)$_2$(mnt) (8a). TBA[Ir(CO)(PPh$_3$)(mnt)] 0.135 g, 0.157 mmol) was placed in a flask and dissolved in 4 mL of acetone. Bromine, 8 μL (0.157 mmol), was then added. The solution turned pale orange, then black, and after stirring for ~5 min, back to orange. The solution was stirred for 2 h, and an acetone solution of PPh$_3$ (0.041 g, 0.157 mmol) was added. The resulting orange solution was stirred for 30 min and concentrated. 2-Propanol was added, and the resultant solution was concentrated and stored at −20 °C overnight. The orange precipitate was suction filtered and washed with hexanes. Yield, 80%. Anal. Calcd for $IrC_{41}H_{30}BrN_2OP_2S_2$: C, 51.04; H, 3.13; Br, 8.29; N, 2.90; P, 6.42. Found: C, 50.88; H, 3.42; Br, 8.09; N, 2.81; P, 5.95.

Physical Measurements. ^{1}H NMR spectra were recorded on a Bruker WH-400 spectrometer at 400.13 MHz. Chemical shifts were calculated from the residual proton resonance of the solvent: benzene, 7.15 ppm; chloroform, 7.24 ppm; acetone, 2.04 ppm. ^{31}P NMR spectra were recorded on the same instrument using a 5-mm ^{1}H/^{31}P probe at 162.35 MHz. Chemical shifts are reported using an external standard of 85% H_3PO_4 as zero. ^{13}C NMR spectra were recorded on the same spectrometer using a 5-mm probe at 100.62 MHz. Chemical shifts are reported in ppm downfield of TMS but were calculated on the basis of the ^{13}C resonance of benzene solvent at 128.3 ppm.

Infrared spectra were obtained from KBr pellets on a Mattson Sirius 100 FT-IR spectrometer and a Perkin-Elmer 467 spectrophotometer. Electronic spectra were recorded on a Perkin-Elmer 330 spectrophotometer. Emission and excitation spectra were recorded on either a Perkin-Elmer MPF-44A fluorescence spectrophotometer (R 446 F photomultiplier tube) equipped with a Perkin-Elmer phosphorescence accessory 063-0504 or a Spex Fluorolog fluorimeter. Solid samples were spread on a Pyrex microscope slide and covered with a cover glass. Spectra at 77 K were obtained from samples placed in a liquid nitrogen Dewar having flat quartz windows.

Gas chromatography was carried out on a Hewlett-Packard 5730A gas chromatograph equipped with an HP 3380A automatic integrator using a 12-ft apiezon on chemisorb column at 150 °C with the flame ionization detector at 200 °C for solution samples. Gas samples were run on a Hewlett-Packard 5700A gas chromatograph equipped with an HP 3380A automatic integrator using a 12-ft Poropak Q column at 43 °C with a thermal conductivity detector at 100 °C. Mass spectra were recorded on a DuPont 21-490 B mass spectrometer.

Photolysis Experiments. Samples for photolysis were prepared by vacuum transferring 0.4 mL of deuterated solvent into a 5-mm NMR tube containing ~2 mg of sample. The sample was subjected to three freeze–pump–thaw cycles and flame sealed. In experiments where radical scavengers or traps and/or excess ligand were added, the sample was made up in the hood and then placed on the vacuum line for three freeze–pump–thaw cycles.

Photolyses were carried out using an Oriel 220 W MP mercury/xenon arc lamp with focusing lens and 350-500-nm band pass filter. The progress of the reaction was monitored by ^{1}H and ^{31}P NMR spectroscopies. The products were compared to authentic samples, independently prepared, by NMR spectroscopy, gas chromatography, and, for methyl bromide, mass spectrometry.

Photolysis of IrMe(CO)(PPh$_3$)$_2$(mnt) (1a) and *n*-Propyl Thiol in the Presence of ^{13}CO. Identical samples were prepared by making a stock solution of 4 mg of **1a** in 1 mL of benzene-d_6 and adding 6 equiv of *n*-propanethiol. A 0.4-mL aliquot of the solution was placed in each of two NMR tubes attached to a high vacuum line and subjected to three freeze–pump–thaw cycles. A pressure of 200 Torr of ^{13}CO was then placed over each solution. After being flame sealed, the samples were kept at 77 K until the initial spectrum was taken. Initial ^{1}H NMR and ^{31}P NMR spectra of the dark thermal control and the photolysis sample were recorded. Spectra were recorded after 1, 4, 5, 10, 15, and 25 min of photolysis and compared to those of the dark control.

Photolysis of IrMe(CO)(PPh$_3$)$_2$(mnt) (1a) in the Presence of ^{13}CO. Samples and photolysis were carried out in the same manner as for **1a** above. Spectra were recorded after 30, 60, 120, and 180 min and compared to those of the dark control.

Photolysis of IrEt(CO)(PPh$_3$)$_2$(mnt) (2a) in the Presence of ^{13}CO. Samples and photolysis were carried out in the same manner as for **1a** above. Spectra were recorded after 1, 2, 3, 4, and 5 min and compared to those of the dark control.

Quantum Yield of Ir–Me Bond Homolysis. A stock solution of 14.4 mg of **1a** in 10 mL of CH_2Cl_2 was prepared, and 58 μL of *n*-propanethiol was added. This concentration ensured an absorbance of 1 or greater for the 350-500-nm range of light used. A 4.0-mL aliquot of the solution was placed in a quartz 1-cm cell fitted with a degassing stem, and the sample was degassed under a slow purge of N$_2$ for 20 min before being photolyzed. The sample was protected from light during preparation and any sampling manipulations. The light from the lamp was masked so that it fell only on the sample. Two series of photolyses were performed with sampling after 10, 20.3, 26.7, 26.7, and 46.7 min for series 1 and 10, 20.7, 35.7, 50.7, and 70 min for series 2. Initial spectra were recorded before the samples were photolyzed. After photolysis, 0.03–mL aliquots of the solution were removed and the FT-IR spectrum recorded. Spectra were obtained by recording a sample spectrum and subtracting a solvent spectrum (CH_2Cl_2 plus *n*-propanethiol) that had been previously recorded in the same 0.1-mm CaF$_2$ cell. The area of interest for the absorbance subtraction was 2250–1850 cm^{-1} with ν_{CO} for **1a** measured as 2012 cm^{-1}. The absorbance for each sample was corrected to a base line of zero to ensure an accurate measurement. The absorbance was converted to concentration by comparison to a Beer's Law plot of absorbance versus concentration of **1a**.

The intensity of the lamp was measured before photolyses, between the photolysis series, and after photolyses using Reinecke's salt, [KCr(NH$_3$)$_2$(SCN)$_4$], as an actinometer.[15] A solution of Reinecke's salt, 0.4 g in 25 mL of distilled water, was prepared; this concentration assured total absorption of the lamp light. All preparations and samplings were protected from the light. Aliquots of 4.00 ± 0.02 mL of solution were placed in 1-cm quartz cells and degassed with N$_2$ for 20 min before being photolyzed for 100 s. Two side-by-side samples were photolyzed for each determination. After photolysis, 1.00 ± 0.02 mL of the solution was diluted to 10.00 ± 0.02 mL with 0.1 M Fe(NO$_3$)$_3$ in 0.5 M HClO$_4$; a dark blank was also prepared. The thiocyanate concentration was then determined by measuring the absorbance at 450 nm, where ϵ_{FeSCN} is 4.3 × 10^3 L mol^{-1} cm^{-1}.

Quantum Yield of β-Elimination of IrEt(CO)(PPh$_3$)$_2$(mnt). Method 1. Three samples of known concentration of IrEt(CO)(PPh$_3$)$_2$(mnt) (**2a**) in benzene-d_6 were prepared immediately prior to photolysis: 7.3 mg/5.0 mL; 7.2 mg/5.0 mL; and 6.7 mg/5.0 mL. Aliquots of 4.0 mL each of **2a** and a Reinecke's salt solution were placed in individual 1-cm quartz cells and degassed, the salt by bubbling N$_2$ through the sample for 20 min and the solution of **2a** by three freeze–pump–thaw cycles on the high vacuum line. The two cells were fastened side-by-side and photolyzed for 60 s. All preparations and manipulations were protected from light prior to photolysis.

Concentrations of the iridium hydride complex **5a** were measured by ^{1}H NMR and compared to an internal standard. Aliquots of 0.50 mL of the solution were used for each NMR spectrum. An initial spectrum

Table 1. Crystallographic Data for Ir(CH_3)(CO)(PPh_3)$_2$(mnt) (**1a**)[a]

chemical formula	$IrC_{42}H_{33}N_2OP_2S_2$
formula weight	900.02
lattice type	triclinic
space group	$P\bar{1}$
Z	2
a, Å	13.178(4)
b, Å	13.670(4)
c, Å	12.592(2)
α, deg	105.03(2)
β, deg	115.42(2)
γ, deg	95.72(2)
V, Å^3	1919.9
ρ_{calc}, g/cm^3	1.557
T, °C	−20
μ, cm^{-1}	36.84
λ (Mo Kα, graphite monochromated), Å	0.710 73
$R(F_o)$	0.020
$R_w(F_o)$	0.028

[a] $R_1 = \{\Sigma\|F_o| - |F_c\|\}/\{\Sigma|F_o|\}$; $R_2 = [\Sigma w(|F_o| - |F_c|)^2]^{1/2}/\{\Sigma wF_o^2\}$, where $w = [\sigma^2(F_o) + (\rho F_o^2)^2]^{1/2}$ for the non-Poisson contribution weighting scheme. The quantity minimized was $\Sigma w(|F_o| - |F_c|)^2$. Source of scattering factors f_o, f', f'': Cromer, D. T.; Waber, J. T. *International Tables for X-Ray Crystallography*; Kynoch Press: Birmingham, England, 1974; Vol. IV, Tables 2.2B and 2.3.1.

was recorded immediately after mixing, and a final spectrum was recorded after photolysis. Concentration of free SCN^- was determined as described above.

Method 2. A comparison quantum yield was determined similar to the method used for Ir–Me bond homolysis. The concentration of **5a** was determined by ^1H NMR spectroscopy using 0.5-mL liquots of sample. Reinecke's solution was photolyzed before the ethyl complex for 120 s and after the ethyl complex for 100 s. The sample of **2a** contained 27.3 mg in 25.0 mL of benzene-d_6 and was photolyzed for 60, 120, and 166 s.

Luminescence Quenching of IrMe(CO)(PPh$_3$)$_2$(mnt). A stock solution of 13.9 mg of IrMe(CO)(PPh_3)$_2$(mnt) in 25.0 mL of CH_2Cl_2 was prepared. The stock solution was used to prepare 4 mL of sample at 0.28 mM concentration by a 1:1 dilution with CH_2Cl_2 solvent. The sample was degassed with a slow purge of N_2 for 20 min, and an emission spectrum was recorded. Varying amounts of the stock solution of **1a**, a second stock solution of *n*-propanethiol (25 μL in 10.0 mL of CH_2Cl_2), and CH_2Cl_2 were combined to produce samples having 0.28 mM concentration of **1a** and 1, 5, and 50 equiv of the thiol. Additional samples containing 500 and 1000 equiv of thiol were made by adding the appropriate amount of *n*-propanethiol to the 0.28 mM solution of **1a**. A spectrum of the iridium sample without the thiol was recorded between each thiol-containing sample to ensure the constancy of fluorimeter response.

Thermal Reaction of IrEt(CO)(PPh$_3$)$_2$(mnt) (2a). A sample of 4 mg of **2a** in 1 mL of benzene-d_6 was prepared, and two NMR samples of 0.4 mL each were degassed under vacuum and flame sealed. Initial spectra were recorded, and one sample was maintained at ambient temperature and the other placed in an 80 °C oil bath. Both were protected from light. Spectra were recorded after 5, 10, and 15 min for the 80 °C sample and after 0.5, 4, 12, and 14 h for the room temperature sample.

Structure Determination of IrMe(CO(PPh$_3$)$_2$(mnt). A crystal measuring 0.1 × 0.1 × 0.1 mm^3, grown from an NMR sample, was found to be triclinic, crystallizing in space group $P\bar{1}$ with cell dimensions a = 13.178(4) Å, b = 13.670(4) Å, c = 12.592(2) Å, α = 105.03(2)°, β = 115.42(2)°, γ = 95.72(2)°, V = 1919.9 Å^3; Z = 2, d_{calcd} = 1.557 g cm^{-3}. An Enraf-Nonius CAD4 diffractometer with graphite monochromator and Mo Kα radiation (λ = 0.710 73 Å) was used for data collection. A total of 6298 unique reflections ($h, \pm k, \pm l$, 4° < 2θ < 45°) were measured by the $\theta/2\theta$ techniques with a scan range of 0.7 + 0.35(tan θ) and a variable scan rate of 1.2–20 deg/min. All data reduction, absorption, least-squares, and Fourier calculations were carried out using the TEXSAN package of programs (Molecular Structure Corporation) on a Microvax II workstation. Convergence was achieved with R_1 = 0.020, R_2 = 0.028, and GOF = 1.09. All important data collection, unit cell, and refinement parameters are summarized in Table 1.

Results and Discussion

Synthesis and Characterization of IrR(CO)L$_2$(mnt) Complexes. The complexes IrR(CO)L$_2$(mnt), where R = alkyl and L = tertiary phosphine, are synthesized from the anionic square-planar complex [Ir(CO)$_2$(mnt)]$^-$ by a sequence involving ligand substitution of one of the carbonyls, alkylation using RX to give the 5-coordinate neutral species Ir(R(CO)L(mnt), and ligand addition to give the final IrR(CO)L$_2$(mnt) product as shown in eq 1. For L = PPh_3, the 5-coordinate intermediates IrR(CO)L(mnt) (R = Me, Et) may be isolated and characterized, but ligand addition occurs readily to form the more stable 6-coordinate complexes. If the initial substitution of eq 1 is carried out with 1 equiv of L only and the second equivalent of L is added after oxidative addition, the competing reaction of RX with PR'$_3$ to form PPR'$_3^+$X$^-$ is eliminated. For the cases where R = hydride, acetic acid or trifluoroacetic acid replaces alkyl halide as the oxidative addition reagent. Characterization of the IrR(CO)L$_2$(mnt) complexes for R = Me, Et, *n*-Pr, CH_2CN, and H has been achieved by ^1H NMR, ^{31}P NMR, infrared, and electronic spectroscopies and, in selected instances, with elemental analyses. Tables 2 and 3 present the ^1H NMR and infrared spectral data for the IrR(CO)L$_2$(mnt) series.

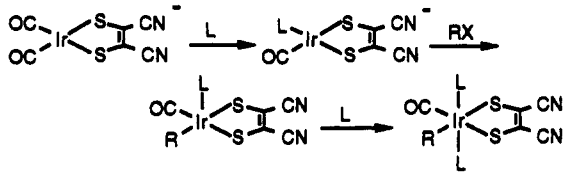

(1)

compd	R	L	compd	R	L
1a	Me	PPh_3	**4a**	CH_2CN	PPh_3
1b	Me	P(*p*-tol)$_3$	**5a**	H	PPh_3
1c	Me	P(*p*-C_6H_4Cl)$_3$	**5b**	H	P(*p*-tol)$_3$
1d	Me	P(*p*-C_6H_4F)$_3$	**5c**	H	PEt_3
1e	Me	P(*p*-C_6H_4(OMe))$_3$	**6a**	5-hexenyl	PPh_3
1f	Me	CN-*t*-Bu	**7a**	2-(allyloxy)ethyl	PPh_3
2a	Et	PPh_3	**8a**	Br	PPh_3
3a	*n*-Pr	PPh_3			

The bromo derivative IrBr(CO)(PPh_3)$_2$(mnt) **8a** is synthesized by the reaction of Br_2 with Ir(CO)(PPh_3)(mnt)$^-$ followed by the addition of 1 equiv of PPh_3. The complex was characterized by elemental analyses and the similarity of its electronic and IR spectroscopic properties with those of the alkyl and hydrido derivatives. The most notable feature about the preparation of **8a** is the fact that the solution turns black before clearing to orange 10 min after the addition or Br_2 to **1a**. The intense color is indicative of a charge-transfer complex and an associated intervalence charge-transfer absorption. The nature of the species that gives rise to this absorption is not established at present but is probably [Br_2···Ir(CO)(PPh_3)(mnt)$^-$] with the optical transition corresponding to electron transfer from Ir(I) to Br_2.

The structure of **1a** as determined by a single crystal structure determination is shown in Figure 1 with important metrical information presented in Tables 4 and 5. The octahedral geometry has methyl and CO ligands trans to the sulfur donors of the mnt ligand and PPh_3 ligands cis to methyl, CO, and mnt in mutually trans positions. An interesting feature of the structure is the difference in length of the two iridium–sulfur bonds, Ir–S$_1$ of 2.442(1) Å and Ir–S$_2$ of 2.372)1 Å; the sulfur atom (S$_1$) trans to the methyl ligand has the longer bond distance, consistent with the structural trans influence of methyl. Previously reported Ir–S bond distances from other complexes containing thiolate or dithiolene ligands are in the range of 2.332–396 Å.[17] The Ir–P bond distances are statistically identical in length, averaging 2.393(1) Å. This value is in agreement with those found in other Ir(III) bis(triphenylphosphine) complexes, including Ir(*p*-CH_3O-

---

(17) (a) Edelman, F.; Roesky, H. W.; Spang, C.; Noltemeyer, M.; Sheldenk, G. M. *Angew. Chem.* **1986**, *98*, 809. (b) Khare, G. P.; Eisenberg, R. *Inorg. Chem.* **1972**, *11*, 1385.

Table 2. ^{1}H NMR^a Spectral Data (δ)^b for the IrR(CO)L$_2$(mnt) Series

complex	δ alkyl	δ ligand
1a, IrMe(CO)(PPh$_3$)$_2$(mnt)	0.39 t (J_{H-P} = 3.7)	7.56 m, 7.43 m
1b, IrMe(CO)(P(*p*-tol)$_3$)$_2$(mnt)	0.35 t (J_{H-P} = 3.7)	7.41 dd (J_{H-P} = 10.0, J_{H-H} = 7.8), 7.18 m, 2.37 s
1c, IrMe(CO)(P(*p*-C$_6$H$_4$Cl)$_3$)$_2$(mnt)	0.34 t (J_{H-P} = 3.8)	7.42 m
1d, IrMe(CO)(P(*p*-C$_6$H$_4$F)$_3$)$_2$(mnt)	0.36 t (J_{H-P} = 3.8)	7.49 m (J_{H-P} = 14.8, J_{H-H} = 7.8), 7.15 dd (J_{H-H} = J_{H-F} = 8.4)
1e, IrMe(CO)(P(*p*-C$_6$H$_4$(OMe))$_3$)$_2$(mnt)	0.39 t (J_{H-P} = 3.5)	7.44 m (J_{H-P} = 9.0, J_{H-H} = 8.4), 6.90 d (J_{H-H} = 8.4), 3.78 s
1f, IrMe(CO)(*t*-BuNC)$_2$(mnt)	0.64 s	1.58 s, 1.50 s
2a, IrEt(CO)(PPh$_3$)$_2$(mnt)	2.69 m, 0.68 t (J_{H-H} = 7.3)	7.60 m, 7.45 m, 7.39 m
3a, Ir(*n*-Pr)(CO)(PPh$_3$)$_2$(mnt)	1.31 m, 0.93 m, 0.05 t (J_{H-H} = 6.8)	7.63 m, 7.44 m, 7.40 m
4a, Ir(CH2CN)(CO)(PPh$_3$)$_2$(mnt)	1.58 t (J_{H-P} = 4.5)	7.64 m, 7.51 m, 7.45 m
5a, IrH(CO)(PPh$_3$)$_2$(mnt)^c	−10.24 t (J_{H-P} = 10.6)	7.72 m, 6.99 m
5b, IrH(CO)(P(*p*-tol)$_3$)$_2$(mnt)	−10.84 t (J_{H-P} = 10.9)	7.49 dt, (J_{H-P} = 5.2, J_{H-H} = 7.9), 7.19 m, 2.13 s
5c, IrH(CO)(PEt$_3$)$_2$(mnt)	−12.60 t (J_{H-P} = 12.0)	1.94 m, 1.08 dt (J_{H-P} = 8.2, J_{H-H} = 7.6)
6a, Ir(5-hexenyl)(CO)(PPh$_3$)$_2$(mnt)^c	5.50 m, 4.88 d (J_{H-H} = 3.4), 4.80 s, 1.55 m, 0.85 m, 0.50 m	7.72 m, 6.98 m
7a, Ir(2-(allyloxy)ethyl)(CO)(PPh$_3$)$_2$(mnt)^c	5.68 m, 5.00 AB q (J_{H-H} = 17.4), 4.48 AB q (J_{H-H} = 10.5), 3.35 br d (J_{H-H} = 5.2), 3.08 t (J_{H-H} = 7.2), 2.15 m	7.72 m, 6.98 m
8a, IrBr(CO)(PPh$_3$)$_2$(mnt)^c		7.87 m, 6.97 m

^{a} 400 MHz, CDCl$_3$ solutions except where noted. ^{b} Chemical shift values are reported in ppm, coupling constants in parentheses are in hetz. Abbreviations: s, singlet; d, doublet; t, triplet; q, quartet; m, multiplet; br, broad. ^{c} C$_6$D$_6$ solutions.

Table 3. Selected Infrared Spectral Data^a for the IrR(CO)L$_2$(mnt) Series

complex	ν_{CO}	ν_{CN}	ν_{IrH}
1a, IrMe(CO)(PPh$_3$)$_2$(mnt)	2017	2201	
1b, IrMe(CO)(P(*p*-tol)$_3$)$_2$(mnt)	2011	2200	
1c, IrMe(CO)(P(*p*-C$_6$H$_4$Cl)$_3$)$_2$(mnt)	2027	2202	
1d, IrMe(CO)(P(*p*-C$_6$H$_4$F)$_3$)$_2$(mnt)	2020	2200	
1e, IrMe(CO)(P(*p*-C$_6$H$_4$(OMe))$_3$)$_2$(mnt)	2016	2201	
1f, IrMe(CO)(*t*-BuNC)$_2$(mnt)	2061	2205	
2a, IrEt(CO)(PPh$_3$)$_2$(mnt)	2015	2200	
3a, Ir(*n*-Pr)(CO)(PPh$_3$)$_2$(mnt)	2015	2198	
4a, Ir(CH$_2$CN)(CO)(PPh$_3$)$_2$(mnt)	2044	2202,^{b} 2211^c	
5a, IrH(CO)(PPh$_3$)$_2$(mnt)	2043	2194	2138
5b, IrH(CO)(P(*p*-tol)$_3$)$_2$(mnt)	2035	2204	2120
5c, IrH(CO)(PEt$_3$)$_2$(mnt)	2031	2197	2121
6a, Ir(5-hexenyl)(CO)(PPh$_3$)$_2$(mnt)	2015	2201	
7a, Ir(2-(allyloxy)ethyl)(CO)(PPh$_3$)$_2$(mnt)	2017	2201	
8a, IrBr(CO)(PPh$_3$)$_2$(mnt)	2054	2198	

^{a} All spectra obtained from KBr pellets; wavenumbers are in cm^{-1}. ^{b} mnt stretching. ^{c} CH$_2$CN stretching.

C$_6$H$_3$NNH)(H)(I)(PPh$_3$)$_2$,[18] Ir(Cl)(H)(η^3-C$_3$H$_4$(1-Ph))(PPh$_3$)$_2$[19] and Ir(bta)(CO)(PPh$_3$)$_2$ (bta = benzotriazenide).[20] The Ir–carbonyl (C$_5$) bond distance is 1.859 Å, which also agrees with previously reported values.[17b,18,20] The most important distance in the structure is that of the Ir–Me bond, which is 2.143(5) Å. While mononuclear Ir alkyl complexes have been reported previously, few structures have been determined crystallographically. Tulip and Thorn have reported the crystal structure of Ir(Et)(Br)$_2$(PMe$_3$)$_3$, with an Ir–C bond distance of 2.123(5) Å,[21] while an iridium phenyl complex, Ir(Ph)(Br)$_2$(CO)(PEt$_3$)$_2$, has been characterized structurally and found to have an Ir–C bond distance of 2.132(10) Å.[22] Although the Ir–Me bond distance in **1a** is slightly longer than those found in the Ir–Et and Ir–Ph complexes, it appears to be not statistically significant. All of the other bond distances and angles appear normal for mononuclear iridium carbonyl complexes.

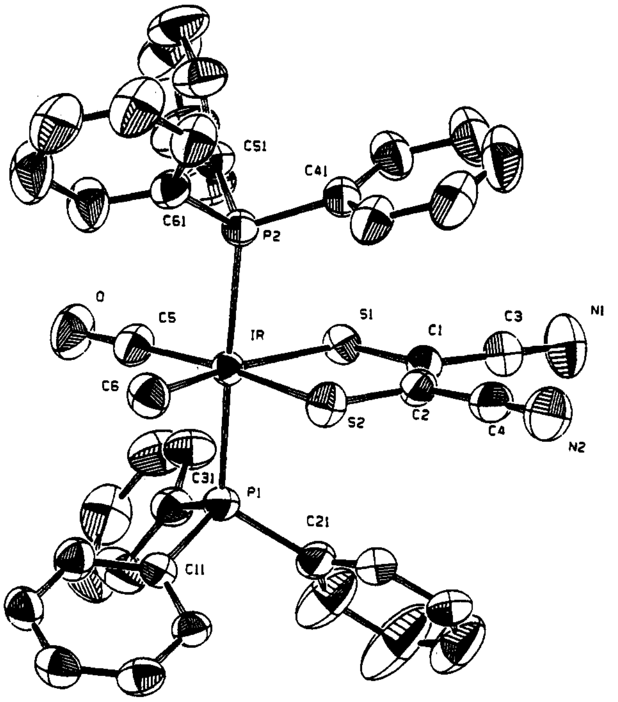

Figure 1. Molecular structure and selected atom numbering of the non-hydrogen atoms (ORTEP diagram, 50% thermal ellipsoids) of IrMe(CO)(PPh$_3$)$_2$(mnt) (**1a**).

Table 4. Selected Intramolecular Bond Distances (Å) for **1a**

atoms	distance	atoms	distance	atoms	distance
Ir–S1	2.442(1)	S2–C2	1.736(5)	O–C5	1.135(5)
Ir–S2	2.372(1)	P1–C11	1.815(4)	N1–C3	1.137(7)
Ir–P1	2.393(1)	P1–C21	1.831(5)	N2–C4	1.134(6)
Ir–P2	2.393(1)	P1–C31	1.831(5)	C1–C2	1.353(6)
Ir–C5	1.859(5)	P2–C41	1.812(4)	C1–C3	1.427(7)
Ir–C6	2.143(5)	P2–C51	1.838(5)	C2–C4	1.442(6)
S1–C1	1.745(4)	P2–C61	1.830(5)		

The ^{1}H NMR spectrum of **1a** exhibits a triplet with J_{PH} of 3.6 Hz, consistent with two equivalent phosphorus donors cis to the methyl ligand, as found in the solid-state structure. The ^{1}H NMR spectra of the other methyl complexes **1b–e** also have triplets with similar coupling constants, indicating coordination geometries identical to that of **1a**. The hydride complexes **5a–c** also exhibit triplet coupling in the hydride resonances, in accord with the hydride ligand cis to two equivalent phosphines, while the infrared results indicate that the hydride and CO ligands are not mutually

---

(18) Belton, P. L.; Demartin, F. M.; Manassero, M.; Sansoni, M. *J. Organomet. Chem.* **1978**, *157*, 209.

(19) Tulip, T. H.; Ibers, J. A. *J. Am. Chem. Soc.* **1979**, *101*, 4201.

(20) Ibers, J. A.; Siedel, A. R. *Inorg. Chem.* **1978**, *17*, 3026.

(21) Thorn, D. L.; Tulip, T. H. *J. Am. Chem. Soc.* **1981**, *103*, 5984.

(22) Behrens, U.; Dahlenburg, A. *J. Organomet. Chem.* **1976**, *116*, 103.

Table 5. Selected Intramolecular Bond Angles (deg) for **1a**

atoms	angle	atoms	angle
S1–Ir–S2	87.66(5)	Ir–P2–C61	116.8(2)
S1–Ir–P1	88.08(4)	C41–P2–C51	104.0(2)
S1–Ir–P2	85.85(4)	C41–P2–C61	106.2(2)
S1–Ir–C5	105.8(2)	C51–P2–C61	100.3(2)
S1–Ir–C6	167.8(1)	S1–C1–C2	124.9(3)
S2–Ir–P1	92.61(5)	S1–C1–C3	114.4(4)
S2–Ir–P2	91.30(5)	C2–C1–C3	120.6(4)
S2–Ir–C5	166.6(2)	S2–C2–C1	124.4(3)
S2–Ir–C6	80.2(1)	S2–C2–C4	115.5(4)
P1–Ir–P2	172.65(4)	C1–C2–C4	120.1(4)
P1–Ir–C5	88.2(1)	N1–C3–C1	178.0(6)
P1–Ir–C6	92.6(1)	N2–C4–C2	178.0(6)
P2–Ir–C5	89.5(1)	Ir–C5–O	173.7(5)
P2–Ir–C6	94.2(1)	P1–C11–C12	119.2(3)
C5–Ir–C6	86.4(2)	P1–C11–C16	122.5(3)
Ir–S1–C1	100.3(2)	P1–C21–C22	119.5(4)
Ir–S2–C2	102.5(2)	P1–C21–C26	120.9(5)
Ir–P1–C11	113.2(1)	P1–C31–C32	120.3(4)
Ir–P1–C21	119.8(2)	P1–C31–C36	122.0(4)
Ir–P1–C31	111.5(2)	P2–C41–C42	119.9(4)
C11–P1–C21	105.9(2)	P2–C41–C46	120.4(4)
C11–P1–C31	103.5(2)	P2–C51–C52	118.8(4)
C21–P1–C31	101.1(2)	P2–C51–C56	123.7(4)
Ir–P2–C41	114.6(1)	P2–C61–C62	124.3(4)
Ir–P2–C51	113.2(1)	P2–C61–C66	117.9(4)

trans. These observations are consistent with the hydride complexes **5a–c** also having the same geometry as **1e**. The triphenylphosphine complexes **1a–5a** have similar ^{1}H NMR spectra in C_6D_6 for the phenyl region, a multiplet at about δ 7.7 for the ortho phenyl protons and another multiplet at δ 7.0 for the meta and para protons. The bis-isocyanide complex **1f** exhibits a singlet for the methyl resonance and two other singlets for the *tert*-butyl isocyanide ligands. The inequivalency of the isocyanide ligands suggests a slightly different coordination geometry for **1f** from that shown in Figure 1, most probably one with the isocyanide ligands cis to each other.

The infrared spectra of the $IrR(CO)L_2(mnt)$ complexes all have ν_{CN} at about 2200 cm^{-1}. The carbonyl stretching frequency, ν_{CO}, varies with donor ability of the phosphine ligand, ranging from 2011 cm^{-1} for **1b** to 2027 cm^{-1} for **1c** (see Table 3). The variation correlates with Hammett's σ parameters and is consistent with the notion that better donating ligands increase the electron density on the metal center, leading to greater Ir → CO π-back-bonding and lower ν_{CO}.[23] The isocyanide-containing complex **1f** has ν_{CO} of 2061 cm^{-1}. This higher stretching frequency may be explained by the greater π-acidity of isocyanide relative to phosphine donor ligands.[23] There is not as much variation in ν_{CO} of the alkyl complexes **1a–3a**, but the methylcyano complex **4a** exhibits a marked shift to 2044 cm^{-1} attributable to the electron-withdrawing effect of the cyano functionality.

The electronic spectra of the $IrR(CO)L_2(mnt)$ complexes all exhibit an absorption band between 350 and 450 nm with extinction coefficients of (2–5) × 10^3 L mol^{-1} cm^{-1}. Data (λ_{max} and ϵ) for specific compounds measured in acetonitrile are reported in Table 6. While the appearance of the absorption spectrum changes slightly with each compound, there exists in general two closely spaced bands in the visible region with one usually appearing as a shoulder of the other. As an example, compound **1a** exhibits a major absorption band at 417 nm with a minor shoulder at 350 nm, although in other compounds the minor absorption may be red- rather than blue-shifted relative to the major band.

Table 6. Electronic Absorption Spectral Data for the $IrR(CO)L_2(mnt)$ Series[a]

complex	λ_{max}, nm (ϵ_{max}, M^{-1} cm^{-1})
1a, $IrMe(CO)(PPh_3)_2(mnt)$	350 sh, 417 (4100)
1b, $IrMe(CO)(P(p\text{-tol})_3)_2(mnt)$	419 (3900), 442 sh
1c, $IrMe(CO)(P(p\text{-}C_6H_4Cl)_3)_2(mnt)$	386 (3700), 420 (3800)
1d, $IrMe(CO)(P(p\text{-}C_6H_4F)_3)_2(mnt)$	417 (3400)
1e, $IrMe(CO)(P(p\text{-}C_6H_4(OMe))_3)_2(mnt)$	412 (4400), 426 (4100)
1f, $IrMe(CO)(t\text{-}BuNC)_2(mnt)$	368 (7500), 383 (7400), 380 (3400), 406 (3800)
2a, $IrEt(CO)(PPh_3)_2(mnt)$	383 (3600), 434 sh
3a, $Ir(n\text{-}Pr)(CO)(PPh_3)_2(mnt)$	391 (2900)
4a, $Ir(CH_2CN)(CO)(PPh_3)_2(mnt)$	384 (3000), 417 (2600)
5a, $IrH(CO)(PPh_3)_2(mnt)$	414 (6100), 430 sh
5b, $IrH(CO)(P(p\text{-tol})_3)_2(mnt)$	419 (3600), 442 sh
5c, $IrH(CO)(PEt_3)_2(mnt)$	425
8a, $IrBr(CO)(PPh_3)_2(mnt)$	387 (4600), 417 (5400), 492 (1200)

[a] Acetonitrile solvent used for all measurements.

Luminescence of $IrR(CO)L_2(mnt)$ Complexes. All of the compounds emit around 700 nm when excited at 430 nm. The emission has vibronic structure reminiscent of that of the square-planar mnt complexes $[IrL_2(mnt)]^-$ and $PtL_2(mnt)$, where L_2 corresponds to either two neutral electron pair donors such as CO and PR_3 or a bidentate ligand such as 1,5-cyclooctadiene, the α,α'-diimines bpy and phen, and diphosphines.[12,24] The emission data for the complexes are listed in Table 7, and Figure 2 shows emission spectra of $IrMe(CO)(PPh_3)_2(mnt)$ (**1a**) in $CHCl_3$ solution at 298 K and in rigid media (solid and EPA glass) at 77 K. The emission maxima in rigid media are generally blue-shifted and more intense than those in fluid solution.[25,26]

The series **1a–e** exhibits a shift of emission energy from 695 nm for **1d** to 713 nm for **1e**, which correlates roughly with the Hammett σ values for the phosphines. The shifting of emission maxima to lower energy with increasing donating ability of the phosphine is similar to, but not as pronounced as, that described previously for the d^8 Ir(I) complexes $[IrL_2(mnt)]^-$.[12] Based on the similarity of emission structure with that found for $[IrL_2(mnt)]^-$ and $PtL_2(mnt)$ systems and the trend to lower emission energy with increasing ligand donor ability, the emissive state in the $IrR(CO)L_2(mnt)$ complexes is assigned as a charge-transfer state involving a π^* orbital of the mnt ligand. The shift of emission maxima with phosphine donor ability results from the destabilizing influence of phosphine donation on the highest occupied molecular orbital (HOMO), which in the Ir(III) octahedral complexes $IrR(CO)L_2(mnt)$ may be either d_π formally derived from one of the t_{2g} orbitals or σ^b involving the alkyl ligand. While the nature of the HOMO is discussed further below, the lowest unoccupied molecular orbital (LUMO) in these systems is clearly π^*(mnt), which is largely unaffected by variation in phosphine donor ability, leading to the observed spectral shifts.[12]

The luminescence lifetime τ of **1a** in $CHCl_3$ solution at ambient temperature is 35 ns, while the relative quantum yield for emission ϕ_{em} has been determined to be 1.68 × 10^{-4} based on a value of 0.042 for $[Ru(bpy)_3](Cl)_2$ in H_2O at 25 °C.[27] From these results, it is possible to obtain an estimate of the natural radiative lifetime τ_0 for the excited state of **1a** as 208 μs. The emission for **1a** and the other $IrR(CO)L_2(mnt)$ complexes is thus a phosphorescence from an excited state of triplet multiplicity.

In view of the observed photochemistry for $IrR(CO)L_2(mnt)$ described below, which involves metal–carbon bond homolysis,

---

[23] Cotton, F. A.; Wilkinson, G. *Advanced Inorganic Chemistry*, 4th ed.; John Wiley and Sons: New York, 1980.

[24] (a) Zuleta, J. A.; Chesta, C. A.; Eisenberg, R. *J. Am. Chem. Soc.* **1989**, *111*, 8916. (b) Zuleta, J. A.; Burberry, M. S.; Eisenberg, R. *Coord. Chem. Rev.* **1990**, *97*, 47. (c) Zuleta, J. A.; Bevilacqua, J. M.; Eisenberg, R. *Coord. Chem. Rev.* **1991**, *111*, 237. (d) Zuleta, J. A.; Bevilacqua, J. M.; Rehm, J. M.; Eisenberg, R. *Inorg. Chem.* **1992**, *31*, 1332. (e) Bevilacqua, J. M.; Zuleta, J. A.; Eisenberg, R. *Inorg. Chem.* **1993**, *32*, 3689. (f) Bevilacqua, J. M.; Zuleta, J. A., Eisenberg, R. *Inorg. Chem.*, in press.

[25] (a) Geoffroy, G. L.; Wrighton, M. S. *Organometallic Photochemistry*; Academic Press: New York, 1979. (b) Balzani, V.; Carassiti, V. *Photochemistry of Coordination Compounds*; Academic Press: New York, 1970.

[26] (a) Wrighton, M. S.; Morse, D. L. *J. Am. Chem. Soc.* **1974**, *96*, 998. (b) Giordano, P. J.; Fredericks, S. M.; Wrighton, M. S.; Morse, D. L. *J. Am. Chem. Soc.* **1978**, *100*, 2257. (c) Zulu, M. M.; Lees, A. *J. Inorg. Chem.* **1989**, *28*, 85.

[27] Nakamaru, K. *Bull. Chem. Soc. Jpn.* **1982**, *55*, 1639.

Table 7. Electronic Emission Maxima and Vibronic Spacing for the IrR(CO)L$_2$(mnt) Series[a]

complex	λ_{max}, nm (ν, cm^{-1})[b]	$\Delta\nu$, cm^{-1} [b]
1a, IrMe(CO)(PPh$_3$)$_2$(mnt)	713 (14.02), 769 (13.00)	1.02
1b, IrMe(CO)(P(*p*-tol)$_3$)$_2$(mnt)	712 (14.05), 768 (13.02)	1.03
1c, IrMe(CO)(P(*p*-C$_6$H$_4$Cl)$_3$)$_2$(mnt)	697 (14.35), 765 (13.07)	1.28
1d, IrMe(CO)(P(*p*-C$_6$H$_4$F)$_3$)$_2$(mnt)	695 (14.40), 765 (13.07)	1.33
1e, IrMe(CO)(P(*p*-C$_6$H$_4$(OMe))$_3$)$_2$(mnt)	713 (14.02), 765 (13.07)	0.95
1f, IrMe(CO)(*t*-BuNC)$_2$(mnt)	712 (14.04), 760 (13.16)	0.88
2a, IrEt(CO)(PPh$_3$)$_2$(mnt)	705 (14.18), 768 (13.02)	1.16
3a, Ir(*n*-Pr)(CO)(PPh$_3$)$_2$(mnt)	710 (14.08), 766 (13.05)	1.03
4a, Ir(CH$_2$CN)(CO)(PPh$_3$)$_2$(mnt)	695 (14.39), 763 (13.11)	1.28
5a, IrH(CO)(PPh$_3$)$_2$(mnt)	708 (14.12), 768 (13.02)	1.10
5b, IrH(CO)(P(*p*-tol)$_3$)$_2$(mnt)	712 (14.04), 770 (12.99)	1.05
5c, IrH(CO)(PEt$_3$)$_2$(mnt)	705 (14.18), 780 (12.82)	1.36
6a, Ir(5-hexenyl)(CO)(PPh$_3$)$_2$(mnt)	706 (14.16), 766 (13.05)	1.11
7a, Ir(2-(allyloxy)ethyl)(CO)(PPh$_3$)$_2$(mnt)	704 (14.20), 766 (13.05)	1.15
8a, IrBr(CO)(PPh$_3$)$_2$(mnt)[c]		

[a] Chloroform solvent used for all fluid solution measurements. [b] Values in parentheses are reported in wavenumbers, ×10^3 cm^{-1}. [c] No emission observed.

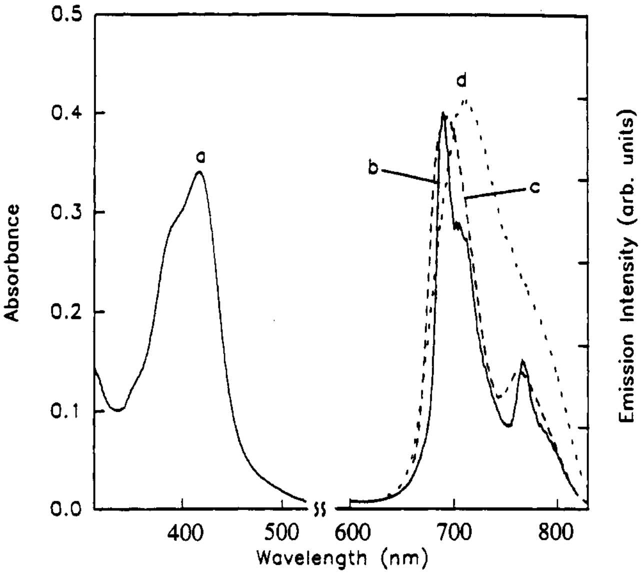

Figure 2. Emission and absorption spectra of IrMe(CO)(PPh$_3$)$_2$(mnt) (**1a**). Intensity expressed in arbitrary units. Spectrum a is the electronic absorption in chloroform; spectra b, c, and d are emission spectra with λ_{exc} at 440 nm. Spectrum b (—) measured in solid state at 77 K; spectrum c (– – –) measured in EPA glass at 77 K; and spectrum d (- - -) measured in CHCl$_3$ solution at room temperature.

the nature of the lowest excited state in these systems is of considerable interest. However, the spectroscopic data obtained to date do not allow an unambiguous assignment to be made. While a charge transfer involving π^*(mnt) seems evident from the common vibronic structure observed in emission from mnt complexes, the nature of the HOMO is uncertain. The possibility that the HOMO corresponds to σ^b for the Ir–alkyl bond rather than d_π receives support from the relatively long natural radiative lifetime of 208 μs observed for **1a**. This value is consistent with less metal character in the HOMO and is significantly longer than the 10–20μs range observed for MLCT states in other Ir(III) complexes.[28] The assignment of σ^b–π^*(mnt) SBLCT (sigma bond-to-ligand charge transfer) excited state is also consistent with homolysis of the Ir–alkyl bond.

States of the SBLCT type have been invoked previously by Wrighton for systems involving Re–Ge and Re–Sn bonds[29] and by Watts for tris-chelated Ir(III) complexes having Ir–Si bonds.[30] However, the assignment has been questioned for the Re–Sn case by Stufkens[31] on the grounds that the σ^b and π^* orbitals would not overlap sufficiently to account for the high intensity of the observed absorption band with ϵ of (4–6) × 10^3. While it has been argued that MLCT states in octaheral d^6 complexes are relatively unreactive in terms of bond homolysis, a recent report by Schanze opines to the contrary.[32] Specifically, Schanze and co-workers find that Re–C bonds in ReR(CO)$_3$(bpy), where R = CH$_3$, CH$_2$Ph, undergo homolysis with high efficiency when photolyzed into the lowest energy absorption band which is assigned by them as MLCT on the basis of absorption and low temperature emission studies.

The shift of emission energy with phosphine donor ability can be rationalized in terms of either a MLCT or a SBLCT emitting state. For the former, increased phosphine donation would cause the energy of the iridium-based d_π HOMO to rise, whereas for the latter, a similar although less pronounced shift in the energy of the Ir–alkyl σ^b orbital, composed of a metal d orbital and a carbon sp^3 hybrid, would be anticipated to occur. In either case, the energy of the π^*(mnt) orbital would not be expected to rise significantly with increased phosphine donation, thus leading to a decreased HOMO–LUMO gap and the observed red shift of emission with greater phosphine donor ability. For an unambiguous assignment of the photochemically active excited state of Ir(CO)L$_2$(mnt), more detailed spectroscopic measurements including lifetime and emission quantum yields as a function of temperature and media remain to be done.

Photochemistry of the IrR(CO)L$_2$(mnt) Series. The photochemistry of IrR(CO)(PPh$_3$)$_2$(mnt) (R = Me, **1a** and R = Et, **2a**) has been studied in detail. All photolyses were followed by NMR spectroscopy, and products were identified by NMR, GC, and, in some instances, mass spectrometry. When the complex IrMe(CO)(PPh$_3$)$_2$(mnt) (**1a**) was photolyzed in benzene-*d*$_6$ solution for 24 h, 95% of the starting material was recovered along with small amounts of the iridium hydride IrH(CO)(PPh$_3$)$_2$(mnt), (**5a**) and toluene. The production of toluene suggested the formation of methyl radicals. The complex **1a** was then photolyzed in the presence of agents to trap any methyl radicals generated. In the presence of 5–10 equiv of *n*-propanethiol, stoichiometric conversion of **1a** to methane, the hydride complex **5a**, and di-*n*-propyl disulfide was observed within 3 h of photolysis, eq 2.

Dark control samples of **1a** and *n*-propanethiol produced no reaction chemistry at ambient temperatures and less than 5% conversion to methane after being heated at 75 °C for 48 h.

---

(28) (a) Ohashi, Y.; Nakamura, J. *Chem. Phys. Lett.* **1984**, *109*, 301. (b) Garces, F. O.; King, K. A.; Wates, R. J. *Inorg. Chem.* **1988**, *27*, 3464. (c) Dedeian, K.; Djurovich, P. I.; Garces, F. O.; Carlson, G.; Watts, R. J *Inorg. Chem.* **1991**, *30*, 1687.

(29) (a) Luong, J. C.; Taltynek, R. A.; Wrighton, M. S. *J. Am. Chem. Soc.* **1979**, *101*, 1597. (b) Luong, J. C.; Taltynek, R. A.; Wrighton, M. S. *J. Am. Chem. Soc.* **1980**, *102*, 7892.

(30) Djurovich, P. I.; Watts, R. J. *Inorg. Chem.* **1993**, *32*, 4861.

(31) Andrea, R. R.; DeLange, W. G. J.; Stufkens, D. J.; Oskam, A. *Inorg. Chim. Acta* **1988**, *149*, 77.

(32) Kirk, L. A.; Burton, R. D.; Schanze, K. S. *Inorg. Chim. Acta* **1993**, *208*, 103.

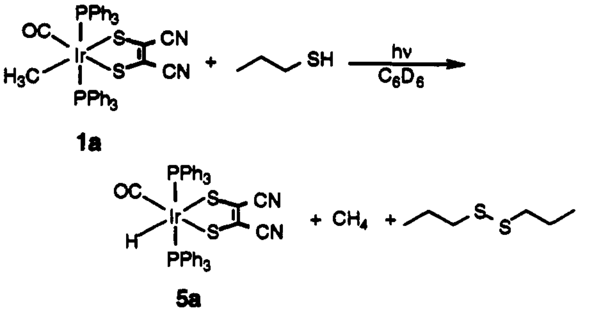

(2)

When **1a** was photolyzed in the presence of 50 equiv of $CDBr_3$, all starting material disappeared within 4.5 h with formation of methyl bromide and $IrBr(CO)(PPh_3)_2(mnt)$ (**8a**), identified by ^1H NMR spectroscopy and gas chromatography. Independent synthesis of **8a** confirmed the assignment. Photolysis of **1a** in the presence of 3 equiv of the stable radical 4-hydroxy-Tempo (4-hydroxy-2,2,6,6-tetramethylpiperidinyloxy) led to complete conversion of starting material to the 4-hydroxy-Tempo methyl ether within 12 h. The results are summarized in Scheme 1.

The quantum yield for eq 2 was determined using 400 equiv of *n*-propanethiol to be 4.7 × 10^{-3}. The large excess of thiol ensured efficient trapping of methyl radicals as they were produced by the photolysis. In the quantum yield determination, disappearance of **1a** was monitored by FT-IR spectroscopy at reaction times less than 1.5 h. The concentration of **1a** for each time interval was determined from a Beer's law plot of the concentration of **1a** versus the absorbance of ν_{CO} at 2021 cm^{-1}. The lamp intensity during photolysis was monitored with Reinecke's salt as an actinometer. Calculation of the quantum yield for photolysis ϕ was made using eq 3, where n_{1a} is the number of moles of **1a**

$$\phi = n_{1a}/I_{0}t \tag{3}$$

consumed, I_0 is the lamp intensity, and t is the time of irradiation.[33] To ensure that the *n*-propanethiol did not affect the excited-state emission, the intensity of the luminescence of **1a** in the presence of *n*-propanethiol was measured. There was no significant quenching of the luminescence in the presence of up to 1000 equiv of the thiol.

In order to determine whether CO dissociation was occurring photochemically in competition with Ir–Me bond homolysis, the photolysis of **1a** was performed in the presence of 200 Torr of ^{13}CO and 6 equiv of *n*-propanethiol. The photolysis was monitored by ^{13}C NMR spectroscopy, and a dark thermal control was used to compare thermal and photochemical ^{13}CO exchange. After 5 min of photolysis, a small amount of CH_4 was observed, but there was no apparent evidence of photochemically promoted ^{13}CO incorporation into **1a**. However, after 20 min, about 10% of the starting material had been consumed, and incorporation of ^{13}CO into both starting complex **1a** and product **5a** was seen by NMR spectroscopy. A thermal reaction of CO with **1a** does occur more slowly, leading to CO exchange in **1a** and formation of the acyl complex $Ir(C(O)Me)(CO)(PPh_3)(mnt)$, analogous to rhodium acyl complexes reported previously.[34] Specifically, when $IrMe(CO)(PPh_3)_2(mnt)$ (**1a**) was placed under 200 Torr of ^{13}CO, there was 10% conversion of **1a** to $Ir(C(O)Me)(CO)(PPh_3)(mnt)$ and free PPh_3 within 3 h in the dark at room temperature, as indicated in eq 4.

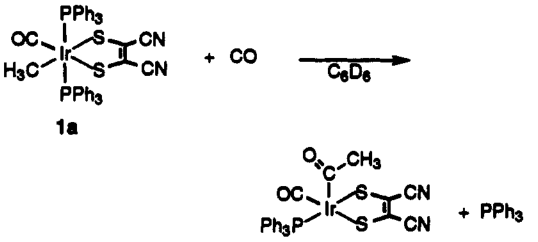

(4)

The relative rates of photochemical and thermal ^{13}CO exchange into **1a** were assessed using two identical samples of **1a** in C_6D_6 under 220 Torr of ^{13}CO. Both the irradiated and the dark control samples were maintained at the same temperature throughout the experiment. After 20 min of photolysis, 55% of the starting material was observed to be ^{13}CO labeled, while for the dark control, only 28% was labeled. After 30 min of photolysis, 79% of the starting material was ^{13}CO enriched, while for the dark sample only 36% was labeled. The results thus suggest that photochemically promoted CO exchange occurs only moderately faster than thermally driven CO exchange. Surprisingly, rapid phosphine exchange was also seen for all of the $IrR(CO)L_2(mnt)$ complexes. In the dark and at room temperature, tertiary phosphine exchange was seen to be facile, occurring at a rate too rapid to measure by conventional kinetics techniques. Despite the rapid phosphine exchange, there was no evidence of phosphine substitution by other ligands such as thiols in the experiments investigating eq 2.

The photochemistry of the ethyl complex $IrEt(CO)(PPh_3)_2(mnt)$ (**2a**) was studied similarly to that of **1a**. When **2a** is photolyzed in benzene, ethylene and the hydride complex **5a** are produced quantitatively *within 5 min* as shown in eq 5. This example of β-elimination, which is also seen with the *n*-propyl complex **3a**, occurs only upon photolysis despite facile tertiary phosphine exchange in the dark at 25 °C. The reaction proceeds much faster than the photochemically promoted CO exchange examined for **1a**.

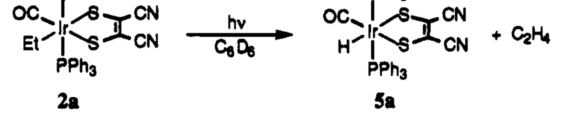

(5)

The quantum yield for appearance of the hydride complex **5a** in eq 5 was found to be 0.3. The concentration of **5a** was determined by ^1H NMR spectroscopy, and determination of ϕ was made by comparison to a Reinecke's salt actinometer during side-by-side photolyses for 60 and 90 s. Equation 6[33] was used to calculate ϕ, where n_{Ir-H} is the number of moles of **5a** produced,

$$\phi_{Ir-H} = n_{Ir-H}\phi_{SCN}/n_{SCN} \tag{6}$$

ϕ_{SCN} is the quantum yield for SCN^- dissociation (0.31) of Reinecke's salt, and n_{SCN} equals the number of moles of SCN^- produced during photolysis of the actinometer. In this experiment, the concentration of **5a** was determined by ^1H NMR spectroscopy. Appearance of **5a** rather than disappearance of **2a** was used to minimize the error from the competing thermal reaction of **2a** to form the acyl complex $Ir(C(O)Et)(PPh_3)_2(mnt)$.

Photolysis of **2a** in the presence of 200 Torr of ^{13}CO showed no incorporation of the label into either starting material or the hydride product during the time of photolysis. This indicates that loss of CO is not the primary photochemical process. In addition, photolysis in the presence of 230 Torr of ^{13}CO and 60 equiv of 1,1-dimethylethanethiol yielded only ethylene and **5a** with no incorporation of label after 1, 3, and 5 min, at which time the reaction was complete. Photolysis in the presence of 300 Torr of CO or 60 equiv of PPh_3 showed no significant slowing of the photolysis rate. It appears that neither CO loss nor phosphine loss plays a part in the photopromoted β-elimination of ethylene from **2a**.

The similarity in emission of the alkyl complexes **1a**, **2a**, and **3a** (λ_{em} of 713, 769 nm for **1a**; 705, 768 nm for **2a**; and 710, 766 nm for **3a**) suggests a common emissive state and similar

---

(33) Calvert, J. G.; Pitts, J. N. *Photochemistry*; John Wiley and Sons: New York, 1966.

(34) (a) Cheng, C.-H.; Spivack, B. D.; Eisenberg, R. *J. Am. Chem. Soc.* 1977, *99*, 3003. (b) Cheng, C.-H.; Eisenberg, R. *Inorg. Chem.* 1979, *18*, 1418.

Scheme 1

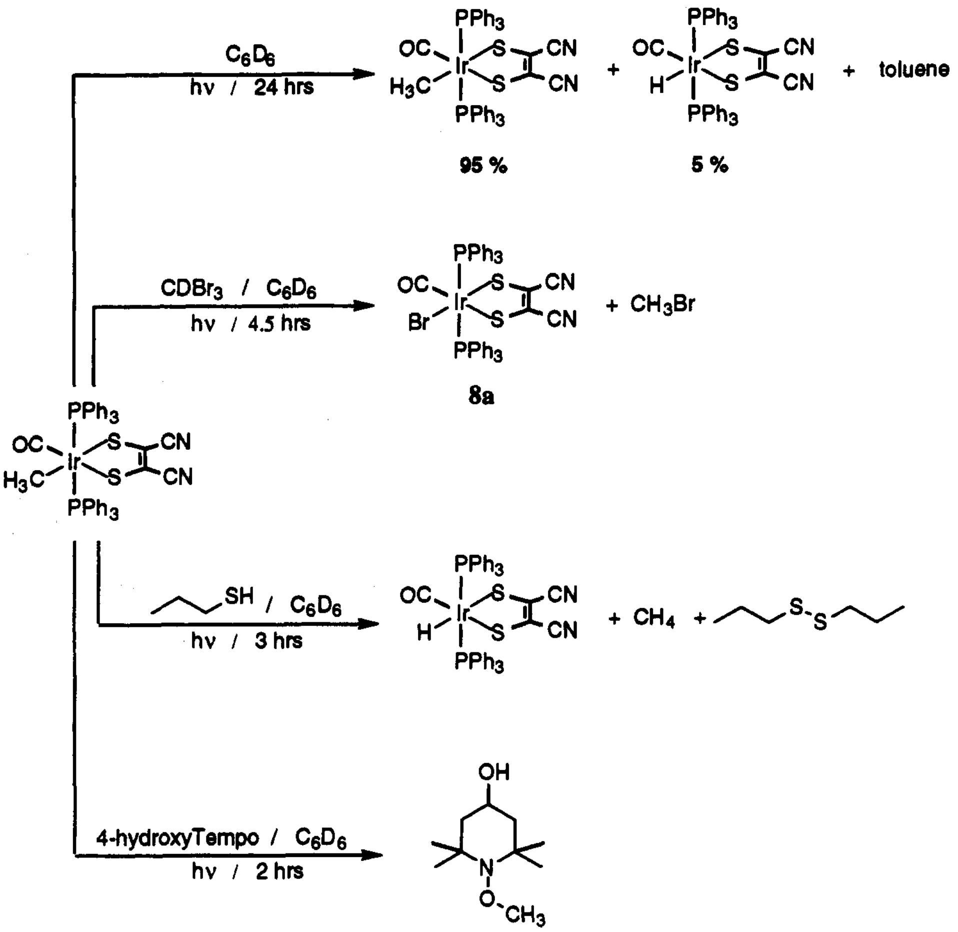

photochemical reactivity of these systems. On the basis of this fact and the observations outlined above, we propose that the β-elimination reaction 5 proceeds by light-driven homolysis of the Ir–Et bond to produce a radical pair comprising Et$^\bullet$ and $^\bullet$Ir(CO)L$_2$(mnt), eq 7, which reacts faster than either geminate recombination or cage separation to transfer an H atom from Et$^\bullet$ to the Ir center, yielding the observed products. Attempts to trap the ethyl radical generated by Ir–ethyl bond homolysis using 1,1-dimethylethanethiol, CDBr$_3$, or 4-hydroxy-Tempo as traps proved unsuccessful.

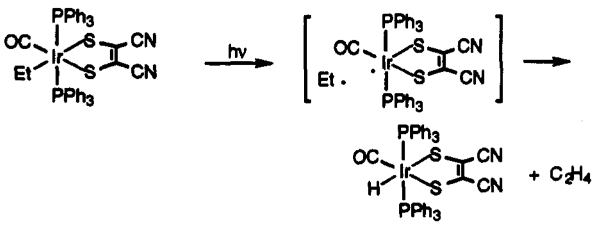

(7)

The photolysis of **2a** was complicated by slower thermal chemistry leading to formation of the acyl complex Ir(C(O)-Et)(PPh$_3$)$_2$(mnt) (**9**), eq 8. For example, **2a**, either along or in the presence of 1,1-dimethylethanethiol, converts to **9** within 3 h at room temperature, while at 80 °C the conversion is complete in 15 min. The conversion to the propionyl complex **9** is stoichiometric, with no ethyl or IrH(CO)(PPh$_3$)$_2$(mnt) (**5a**) complex observed even when the reaction is performed at elevated temperatures.[35]

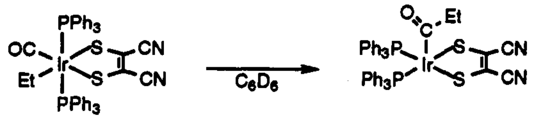

2a **9** (8)

In an attempt to prove a radical mechanism for the photoinduced β-elimination process of eq 7, two iridium alkyl complexes were prepared that upon photolysis would produce an alkyl radical capable of structural rearrangement.[36] In the first instance, Ir(5-hexenyl)(CO)(PPh$_3$)$_2$(mnt) (**6a**) was prepared and characterized. This complex would produce the 5-hexenyl radical upon photolysis, which is known to rearrange to the methylcyclopentyl radical.[37] However, upon photolysis only **5a** and 1,5-hexadiene were produced (eq 9). The second complex synthesized was Ir(1-allyloxy ethyl)(CO)(PPh$_3$)$_2$(mnt) (**7a**), which would generate upon photolysis the 2-(allyloxy)ethyl radical, which rearranges to 2-methylfuran with a rate constant of ~10^7 s^{-1}.[38] Again, only

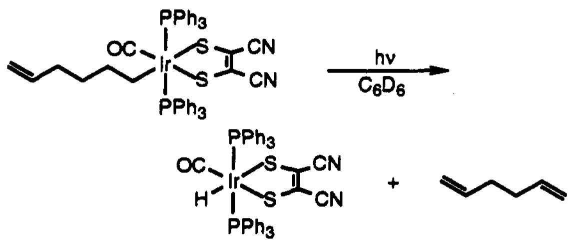

(9)

---

[35] Suardi, G.; Eisenberg, R., to be submitted.

[36] For examples of radical rearrangement reaction used to determine mechanisms in organometallic chemistry, see: (a) Kinney, R. J.; Jones, W. D.; Bergman, R. G. *J. Am. Chem. Soc.* **1978**, *100*, 7902. (b) Ash, C. E.; Hurd, P. W.; Darensbourg, M. Y.; Newcomb, M. *J. Am. Chem. Soc.* **1987**, *109*, 3313.

[37] Griller, D.; Ingold, K. U. *Acc. Chem. Res.* **1980**, *13*, 317.

[38] Beckwith, A. L. J.; Blair, I.; Phillipou, G. *J. Am. Chem. Soc.* **1974**, *96*, 1613.

β-elimination products, **5a** and 2-(allyloxy)ethylene, were seen upon photolysis (eq 10). In both of these cases, the radical rearrangement rate may be too slow if in fact H-atom transfer between the alkyl and iridium radicals occurs rapidly within the radical pair cage. Attempts to synthesize the methylcyclopropyl derivative, which upon homolysis would rearrange to give the ring-opened butenyl radical with a rate constant $\sim 10^8$ s^{-1},[37] were unsuccessful. Further studies to probe the mechanism of this efficient photochemical β-elimination are in progress.

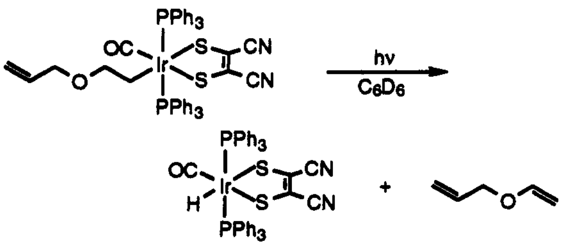

(10)

The large quantum yield for the photochemical reaction of eq 5 stands in contrast with the much less efficient photochemistry of Scheme 1 involving the Me complex **1a**. Since both the Me and Et complexes appear to possess virtually identical electronic structures based on absorption and emission spectroscopies, the difference in photochemical reactivity may seem puzzling at first glance. However, the efficient β-elimination of eq 5 results from the rapid and exothermic transfer of a H-atom from Et$^\bullet$ to $^\bullet$Ir(CO)L_2(mnt) within the radical pair generated by homolysis. It is estimated that the C–H bond energy for the methyl group of an ethyl radical is 38 kcal/mol,[39] which is less than an estimated value of >60 kcal/mol for the Ir–H bond formed in the transfer. On the other hand, for **1a** and other alkyl derivatives of IrR(CO)L_2(mnt) having no β-hydrogens, the in-cage H-atom-transfer route is unavailable, and the system simply undergoes geminate recombination upon homolysis. The quantum yields for the reaction chemistry of Scheme 1 thus reflect the efficiency of cage escape leading to net reaction chemistry relative to geminate recombination to regenerate the alkyl complex IrR(CO)L_2(mnt).

Conclusions

The IrR(CO)L_2(mnt) series of complexes are among the first transition-metal alkyl complexes to luminesce in fluid solution. The luminescence is observed at $\sim$700 nm and is structured similarly to that seen for the square-planar mnt complexes IrLL′(mnt)$^-$ and PtL_2(mnt).[12,24] In the IrR(CO)L_2(mnt) complexes, there is a red shift of emission maxima as the donor ability of the tertiary phosphine ligands increases. The similar structuring of the emission for all mnt complexes and red-shifting of the emission to lower energy with increasing ligand donor ability point to a charge-transfer excited state involving π^*(mnt) as the acceptor orbital or LUMO. The nature of the HOMO in these Ir(III) alkyl complexes may be either d_π or σ^b, leading to assignment of the excited state as either MLCT or SBLCT, respectively. The lifetime of the methyl complex **1a** in fluid solution at ambient temperature has been determined to be 35 ns which, when combined with a fluorescence quantum yield of 1.683×10^{-4}, yields a natural radiative lifetime of 208 μs. This value is consistent with the emissive state having spin-forbidden character in a complex containing a third transition series metal ion.

The photochemistry of the IrMe(CO)(PPh$_3$)$_2$(mnt) has been studied in the absence and presence of radical scavengers. The primary photochemical process is Ir–Me bond homolysis. Confirmation of the occurrence of methyl radical upon photolysis is established by carrying out the reaction in the presence of radical traps or scavengers. In contrast with the results for the methyl complex **1a**, photolysis of IrR(CO)(PPh$_3$)$_2$(mnt), where R contains β-hydrogens, leads exclusively and rapidly to the β-elimination products of olefin and the Ir(III) hydride complex **5a**, even in the presence of a large excess of phosphine or CO. During the time needed for completion of the β-elimination reaction, there is no photochemically promoted ^{13}CO incorporation into the starting alkyl complex or the product. However, attempts at trapping the alkyl radical generated upon photolysis with a radical scanvenger or through radical rearrangement products have proven unsuccessful. The necessity of light for β-elimination, combined with the observation of no significant change in rate for photochemical reaction when excess ligands are present, indicates that β-elimination occurs via an unusual homolytic pathway.

Acknowledgment. We wish to thank the Department of Energy, Division of Chemical Sciences, for support of this research and Johnson Matthey Aesar/Alpha Co. for a generous loan of iridium salts. G.S. gratefully acknowledges the Swiss National Science Foundation for a postdoctoral fellowship. We also wish to thank Professor R. Watts (UC-SB) for helpful comments.

Supplementary Material Available: Complete listing of crystallographic details, bond lengths and bond angles, and positional and anisotropic thermal parameters for **1a** (13 pages); listing of observed and calculated structure factors for **1a** (37 pages). This material is contained in many libraries on microfiche, immediately follows this article in the microfilm version of the journal, and can be ordered from the ACS; see any current masthead page for ordering information.

---

[39] Benson, S. W., *Thermochemical Kinetics*, 2nd ed.; John Wiley and Sons: New York, 1976.